Astron. Astrophys. 142, 393–400 (1985)

ASTRONOMY
AND
ASTROPHYSICS

Effects of CO molecules on the outer solar atmosphere: a time-dependent approach

D. Muchmore and P. Ulmschneider

Institut für Theoretische Astrophysik, Im Neuenheimer Feld 294, D-6900 Heidelberg, Federal Republic of Germany

Received July 6, accepted August 8, 1984

Summary. Carbon monoxide can be an important source of cooling near the solar temperature minimum. We investigate the influence of radiation in the 4.6 μm fundamental vibration-rotation band on the structure of the Sun's outer atmosphere. The model calculations employ a 1–D hydrodynamical code in conjunction with a two-frequency treatment of radiative transfer. Resulting models have a bistable character. Radiative equilibrium atmospheres for $T_{\rm eff} < 5800$ K are dominated in outer layers by CO cooling which draws the temperature down to $T \lesssim 3000$ K. For hooter models, CO plays no important role. The chromosphere adjusts from one state to another in a time of the order of one hour. Acoustic heating destroys CO in the outermost parts of a model but for low and moderately high acoustic fluxes CO continues to dominate the region of the temperature minimum.

Key words: chromosphere – carbon monoxide – radiative hydrodynamics

1. Introduction

Observations of the infrared bands of carbon monoxide in the solar spectrum (Noyes and Hall, 1972; Ayres and Testerman, 1981) have indicated the presence of material at surprisingly low temperatures in the solar atmosphere. In the $\Delta V = 1$ vibration-rotation band of CO, centered at $\lambda = 4.6$ μm, Ayres and Testerman found core brightness temperatures as low as 3700 K for strong lines near the solar limb. This contrasts strikingly with the minimum temperature inferred from other spectral diagnostics. The wings of the Ca II K and Mg II k lines imply a temperature minimum at roughly 4500 K (Ayres and Linsky, 1976), while empirical continuum models (Vernazza et al., 1981) place the temperature minimum around 4200 K.

The very low temperature seen in CO has led to speculations on the influence of CO on the thermal structure of the Sun's outer atmosphere. Ayres (1981) has argued that CO should be a powerful coolant in the neighborhood of the temperature minimum. He suggests that the solar atmosphere may bifurcate into two distinct types of regions – hotter regions with mechanical heating (perhaps magnetic flux tubes) in which CO is dissociated and cooler regions (between the flux tubes) where CO forms and cools the gas to below 4000 K. Kneer (1983) has even argued that the great temperature sensitivity of the CO formation and cooling function may so destabilize the solar atmosphere that no radiative equilibrium is possible. He goes so far as to suggest that the energy balance in the IR bands of CO may account for the chromospheric temperature rise in late-type stars and may also provide the long-sought explanation of the Wilson-Bappu relation.

The purpose of the present paper is to investigate the influence of carbon monoxide using time-dependent radiation hydrodynamic methods. In this approach at every time and height step the mass-, momentum-, and energy conservation equations are consistently solved together with the radiative transfer equation in the optical and the infrared (CO) frequency bands. This approach has the advantage that any instabilities can be followed explicitly and the temporal evolution towards a radiative equilibrium or a dynamical steady state can be directly exhibited. Thus e.g. Kneer's suggestions that equilibrium atmospheres might not exist for stars like the Sun or cooler can be directly tested.

In Sect. 2 we describe our method and the procedure by which we construct atmosphere models. Section 3 discusses radiative equilibrium models. The dynamical response of the atmosphere to disturbances is investigated in Sect. 4. Section 5 gives our conclusions and outlines possible improvements to the current work.

2. Method

2.1. The hydrodynamic code

The method employed here for the hydrodynamical calculation is that of Ulmschneider et al. (1977, 1978) with radiative transfer as described by Kalkofen and Ulmschneider (1977). In this procedure the hydrodynamic equations are solved using the method of characteristics with velocity u, sound speed c, and entropy S as dependent variables of the Lagrangian height a and time t. A time-dependent calculation is started from an initial atmosphere model (which usually is in radiative equilibrium) by modifying the conditions at the lower boundary. This is either done by moving a piston or by perturbing the ingoing radiation field. The only significant change in our present work as compared to the older method is the way in which we treat the upper boundary.

2.2. Upper boundary condition

The so called "transmitting" boundary condition of the older method assumed that the velocity amplitude u is carried unchanged along the C^+-characteristic. The remaining two unknowns S and c are obtained in the usual way by solving the ordinary differential equations along the C^0- and C^+-characteristics, respectively. This assumption works well in cases where disturbances (waves) of considerable amplitude propagate towards

Send offprint requests to: D. Muchmore

the top of the atmosphere. Here the information moves primarily along the C^+-characteristic (cf. Ulmschneider, 1984). We had difficulties with this boundary condition in some cases when velocities were dominated by bulk motions rather than waves. In particular, the difficulties arose when velocities dropped to small values ($u \leqq 10^3\,\mathrm{cm\,s^{-1}}$) with very low outer temperatures ($T < 2000\,\mathrm{K}$). Physically, it is clear that important changes in such cases now occur primarily along the (fluid path) C^0-characteristic. In our present method, therefore, we replace the "transmitting" boundary condition by a condition for c along the C^0-characteristic while computing the remaining unknowns u and S by solving the ordinary differential equations along the C^+- and C^0-characteristics.

From the basic relations between the thermodynamic variables ϱ, c, S we have

$$\frac{\partial c}{\partial t} = \frac{\gamma-1}{2} c\left[\frac{1}{\varrho}\frac{\partial \varrho}{\partial t} + \frac{\mu}{\mathscr{R}}\frac{\partial S}{\partial t}\right], \tag{1}$$

where γ is the ratio of specific heats, μ the mean molecular weight and $\mathscr{R}$ the gas constant. Using the continuity equation in Lagrangian form [Eqs. (2) and (3) of Ulmschneider et al., 1977], we eliminate the density derivative:

$$\frac{\partial c}{\partial t} = \frac{\gamma-1}{2} c\left[\frac{\mu}{\mathscr{R}}\frac{\partial S}{\partial t} - \frac{\varrho}{\varrho_0}\frac{\partial u}{\partial a}\right], \tag{2}$$

where ϱ_0 is the initial density at Lagrangian height a. For the evaluation of c at the top boundary using Eq. (2) along C^0 the value $\frac{\partial u}{\partial a}$ must be known at a mid point. As $u = \mathrm{const}$ along the C^+-characteristic was a good approximation for the "transmitting" boundary, we can consistently estimate $\frac{\partial u}{\partial a}$ along C^0 by advancing it without change parallel to C^+. The outer quantities at the right hand side of Eq. (2) are evaluated at the midpoint along C^0 by averaging between the values at the new and old time levels in successive iterations.

As with the old boundary conditions, acoustic waves are transmitted with good efficiency since $du|_{C^+} = 0$. The new boundary condition has performed well in all cases we have tried. For a train of waves with period 30 s propagating through a model solar atmosphere, the two boundary conditions yield only small differences. For slowly varying, cool atmospheres the new boundary condition appears highly preferable.

2.3. *The treatment of CO*

For the exploratory work we present here, we take the simplest possible model for the radiation field: two frequency bands. One band in the infrared represents all wavelengths $\lambda > 4\,\mu\mathrm{m}$. In this band we use the opacity of the $\Delta V = 1$ vibration-rotation band of CO which consists of a system of largely non-overlapping lines mainly between $4.3\,\mu\mathrm{m} < \lambda < 5.3\,\mu\mathrm{m}$ and decreasing in strength toward longer wavelength. The second frequency band is our "optical" band for all wavelengths $\lambda < 4\,\mu\mathrm{m}$. The opacity here we take from a table of Rosseland mean continuum opacities of Kurucz (1979) for material of solar composition. This opacity arises, of course, primarily from H^-.

To split the two frequency bands, we use a weighting function

$$w(T) = \int_{4\,\mu\mathrm{m}}^{\infty} B_\lambda(T)\,d\lambda / B(T), \tag{3}$$

where B_λ is the Planck function. In practice, we use an approximation to $w(T)$ by fitting the right hand side of Eq. (3) with polynomials in T^{-1}. We use one of two separate polynomials according to whether T is less than or greater than 3000 K and interpolate smoothly between the two between 2900 K and 3100 K. With two such 3rd order polynomials we approximate $w(T)$ to within a few percent for $T = 750$–$11{,}000\,\mathrm{K}$. The LTE source function is then $w(T)B(T)$ in the IR band and $(1-w(T))B(T)$ in the optical band (cf. Mihalas, 1978, p. 208). The lower boundary conditions on the incoming flux (see Ulmschneider et al., 1978) become

$$dI^+ = 3/4\mu w(T_{\mathrm{eff}})B(T_{\mathrm{eff}}) \tag{4}$$

for the IR and

$$dI^+ = 3/4\mu(1-w(T_{\mathrm{eff}}))B(T_{\mathrm{eff}}) \tag{5}$$

for the optical band, where $\mu = 1/\sqrt{3}$ is the angle cosine.

We approximate the CO opacity in a highly simplified manner. Using the molecular constants given by Huber and Herzberg (1979) for $^{12}C^{16}O$ and the oscillator strengths of Kirby-Docken and Liu (1978) we calculate a Planck mean opacity per molecule

$$\kappa_{\mathrm{CO}} = \frac{\pi e^2}{mc}\,\frac{\sum_{V,J}(2J+1)e^{-E_{VJ}/kT}\sum_{\Delta J} f_{V,J,\Delta J}B_\nu(1-e^{-h\nu/kT})}{w(T)B(T)\sum_{V,J}(2J+1)e^{-E_{VJ}/kT}}. \tag{6}$$

V and J are the vibrational and rotational quantum numbers, respectively, and ΔJ takes on the values $+1$ and -1. $f_{V,J,\Delta J}$ is the oscillator strength for the transition from the state $\langle VJ|$ to $|(V+1)(J+\Delta J)\rangle$ which occurs at frequency $\nu = \nu_{V,J,\Delta J}$. $E_{V,J}$ is the energy of the vibration-rotation level V, J. We included a total of 1080 transitions in the summations in Eq. (6). Specifically, these were the 10 lowest V states for all J's up to 49–50 and an additional 10 V states for J's from 0–1 to 3–4. The resulting opacity appears in Fig. 1.

We assume that CO is in LTE and neglect the CO binding energy in the gas dynamics. Equilibrium populations of the energy levels within the molecules should be accurately maintained (Tsuji, 1964; Thompson, 1973). The association-dissociation equilibrium is more questionable. Dynamic processes occur on a variety of time scales some of which could well be shorter than the equilibration time. We do not analyse this question in detail here but merely note that we concentrate primarily on relatively slow processes for which we can argue that the LTE assumption should

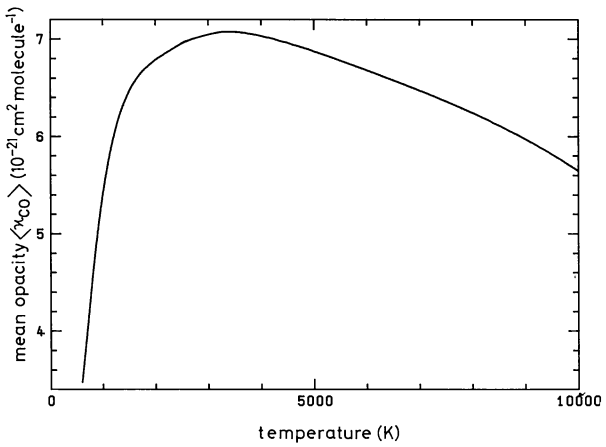

Fig. 1. Planck mean opacity of carbon monoxide

apply. We calculate the CO equilibrium using partition functions provided by Kurucz (1983) for neutral C and O and for CO. We adopt $A_c = 4\,10^{-4}$ and $A_0 = 8\,10^{-4}$ (Ayres and Testerman, 1981) as the abundances of carbon and oxygen.

Approximating the opacity in the IR band by the CO opacity is not strictly correct. When CO forms, its opacity averaged over our IR band is much greater than the Rosseland mean opacity for H^- and atoms so that locally the approximation is very good.

What we lose this way is the radiative interaction between CO in cool regions and other opacity sources in hot regions. Such cases occur here when a hot wave passes through a cooler atmosphere, but since the optical thickness of such a wave is typically of the order of 10^{-5}, the practical significance is negligible. The advantage of this approach is an especially clear separation of effects in the two bands. We have checked the validity of this approximation by running a few test cases with a more realistic opacity $\kappa_{IR} = \kappa_{CO} + \kappa_{opt}$, where κ_{opt} again is the gray continuum opacity. These tests did not show any appreciable differences. Above all, it is clear that the structures of the equilibrium atmospheres remain unaltered.

2.4. *Instability of the cooling function*

Ayres (1981) and Kneer (1983) have emphasized the potential instability seen in the radiative cooling function for an optically thin gas comprised of H^- and CO. With our treatment of the opacities, we can form a comparable cooling function which shows a similar potential instability. For a particular optical depth and a particular incident intensity, a gas is unstable when a perturbation to a lower temperature increases the total radiative cooling rates $d\phi/dT < 0$. Assuming an incident flux of $\sigma T_{\rm eff}^4$ on an element of gas that is completely optically thin,

$$\begin{aligned}\phi &= 4\pi[\kappa_{CO}(B_{CO} - J_{CO}) + \kappa_{opt}(B_{opt} - J_{opt})] \\ &\approx 4\pi\,\kappa_{CO}\{B(T)w(T) - \tfrac{1}{2}B(T_{\rm eff})w(T_{\rm eff})\} \\ &\quad + 4\pi\,\kappa_{opt}\{B(T)[1 - w(T)] - \tfrac{1}{2}B(T_{\rm eff})[1 - w(T_{\rm eff})]\}\,. \end{aligned} \tag{7}$$

Here ϕ is the cooling function. Figure 2 illustrates the regions in parameter space in which $d\phi/dT|_{ad} < 0$ for adiabatic perturbations in two cases: $T_{\rm eff} = 6000$ K and $T_{\rm eff} = 5000$ K. Also shown here is the run of a usual model of the solar atmosphere (Vernazza et al., 1981). The solar temperature minimum falls into the instability region, clearly illustrating the crux of the issues which have been raised by Ayres and by Kneer.

3. Radiative equilibrium atmospheres

In terms of computer time a time-dependent calculation is clearly not the most efficient way to find a radiative equilibrium atmosphere model. However, because a time-dependent computation simulates much more closely the way by which nature achieves radiative equilibrium this method has great advantages.

In particular the question raised by Kneer whether CO may prevent solar-type atmospheres from ever existing in radiative equilibrium is a question which can only be answered in a time-dependent study. A failure in trying to construct models cannot disprove the existence of static equilibrium, it may simply be a failure of the method. A success on the other hand may result in an equilibrium model which is dynamically unstable.

We find that taking CO molecules into account in models for solar-type stars leads to significant changes in the structure of the atmosphere compared with models without CO, but in all cases radiative equilibrium was established. When we begin with an initial gray equilibrium solar atmosphere without CO calculated with the same opacity table which we use here for our optical band, we find that the models with CO come to equilibrium after oscillating for a time on the order of an hour, that is after roughly 25 transit times of the atmosphere. The run of temperature with height of the obtained models is plotted in Fig. 3 for three different effective temperatures near the solar effective temperature. These temperatures were chosen in the range of temperatures observed in granular or intergranular regions on the solar surface.

We note the clearly visible thermal bifurcation in these models which reflects the instability region already described in Fig. 2. There obviously exists an effective temperature T_{cr} such that for $T_{\rm eff} < T_{cr}$, CO forms in the outer atmosphere and depresses the temperature to $T \lesssim 3000$ K. There also exists an effective temperature T'_{cr} such that for $T_{\rm eff} > T'_{cr}$ little or no CO exists in the outer atmosphere and T stays above 4500 K. It is not necessary that $T_{cr} = T'_{cr}$. Conceivably there could exist intermediate effective temperatures for which either of the two types of atmospheric structure would be stable. One sees in Fig. 3 for solar gravity these critical temperatures lie between $T_{\rm eff} = 5770$ and 5900 K. It would be interesting to know more precisely at which $T_{\rm eff}$ CO becomes an important coolant, but that is a question which cannot be answered with our present crude calculation. We can only say that this temperature lies intriguingly close to the solar $T_{\rm eff}$.

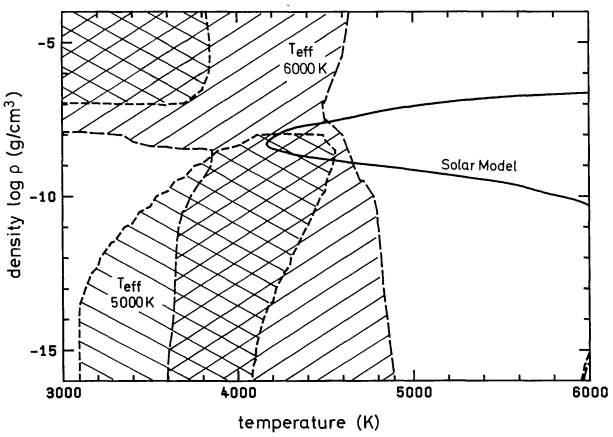

Fig. 2. Unstable regions (hatched) in the T-log ϱ plane for $T_{\rm eff} = 5000$ K and 6000 K. In these regions, the derivative of the cooling function is $d\phi/dT|_{ad} < 0$ [cf. Eq. (7)] and perturbations are radiatively amplified. Also shown is the solar Model C from Vernazza et al. (1981)

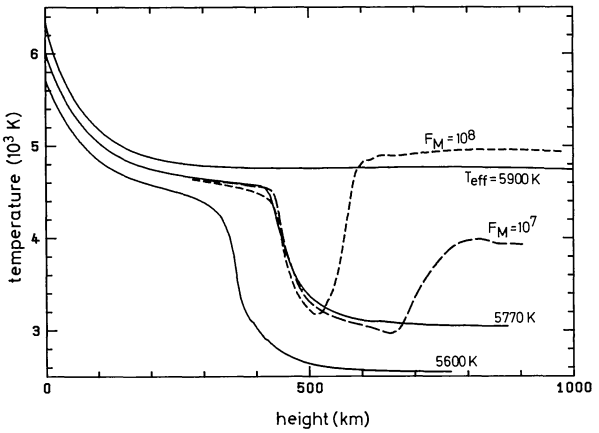

Fig. 3. Temperature stratification in equilibrium models. Solid lines are static models at various $T_{\rm eff}$. Dashed lines are models for $T_{\rm eff} = 5770$ K with steady influx of acoustic waves. The energy flux of the waves in erg cm^{-2} s^{-1} is marked as a parameter

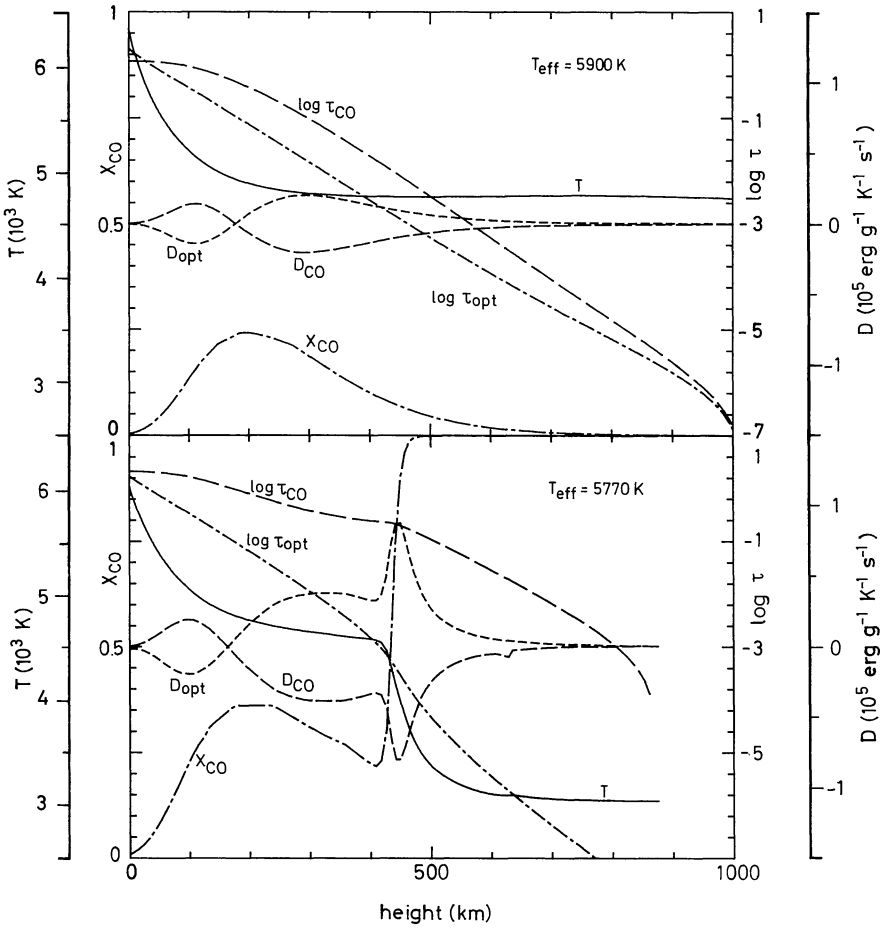

Fig. 4. Structure of equilibrium atmospheres. The radiative damping function $D=\left.\frac{\partial S}{\partial t}\right|_{\text{rad}}$ and $\log\tau$ are shown for each of the two frequency bands, along with the temperature and X_{CO}, the fraction of carbon atoms in CO. Models are for the effective temperatures 5900 and 5770 K

The three models in Fig. 3 extend to different heights, but all represent the same atmospheric mass. This is a natural consequence of the Lagrangian coordinate system used for the calculation. The initial gray solar model (without CO) with a height of 1000 km expands only marginally on being heated to $T_{\text{eff}}=5900$ K. The strong cooling by CO in the models at $T_{\text{eff}}=5770$ and 5600 K leads to appreciable contraction of the atmosphere.

Further details of the structures of these atmospheres are presented in Fig. 4, which shows the optical depth and rate of entropy change for each of our two frequency bands, as well as the temperature and X_{CO}, the fraction of carbon atoms bound in CO molecules. The radiation damping function $D=\left.\frac{\partial S}{\partial t}\right|_{\text{rad}}$ represents the gain of entropy by the gas from the radiation field. Positive values of D correspond to radiative heating, negative ones to radiative cooling. In equilibrium, cooling in the CO band is balanced by heating in the optical bands. Since non-LTE effects in H^- are known to be significant for the thermal structure of the lower chromosphere (Ayres, 1980; Schmitz et al., 1984), the details of the balance found in our LTE calculations should deviate from the true situation. A non-LTE reduction in the H^- opacity would have the effect of moving the level of the CO-produced temperature falloff (for $T_{\text{eff}}<T_{\text{cr}}$) closer to the surface of the star.

The optical depth is much larger in the CO frequency band than in the optical. For $T_{\text{eff}}=5900$ K, τ_{CO} exceeds τ_{opt} by roughly one order of magnitude from $z=100$ to 800 km. $\tau_{\text{opt}}>\tau_{CO}$ only in the layers $z\lesssim 50$ km, where CO dissociates towards the stellar interior. For the cooler models, τ_{CO} is several orders of magnitude larger than τ_{opt} except for the deepest 100 km above the photospheric level. The temperature falloffs caused by CO occur at $\tau_{CO}\sim 0.5$ and $\tau_{CO}\sim 0.3$ for $T_{\text{eff}}=5770$ and 5600 K, respectively, that is at a height where CO can freely radiate into space and thus becomes an important coolant.

4. Atmospheric dynamics

The surfaces of most stars are never truly static; they vary in temperature and pressure on a variety of spatial and temporal scales due to variations in convective cells, radial and non-radial global oscillations, the emergence of concentrated magnetic flux and mechanical heating. The overlying outer atmosphere may or may not have sufficient time to come into equilibrium. In this section we discuss the response of an atmosphere to several simple perturbations.

4.1. Response to an altered surface temperature

To give a feeling for the speed with which radiative equilibrium is established at various heights we discuss in more detail the physical processes which follow after a rapid change of surface temperature. Figure 5 shows a sequence of events which occur when the incident radiation in an atmosphere which initially is in radiative equilibrium at $T_{\text{eff}}=5900$ K is suddenly dropped at the lower (left) boundary to a value corresponding to $T_{\text{eff}}=5600$ K. Temperature fluctuations of this magnitude are observed in granules but occur over longer time scales. Figure 5 shows that both radiative and gas dynamic effects are important.

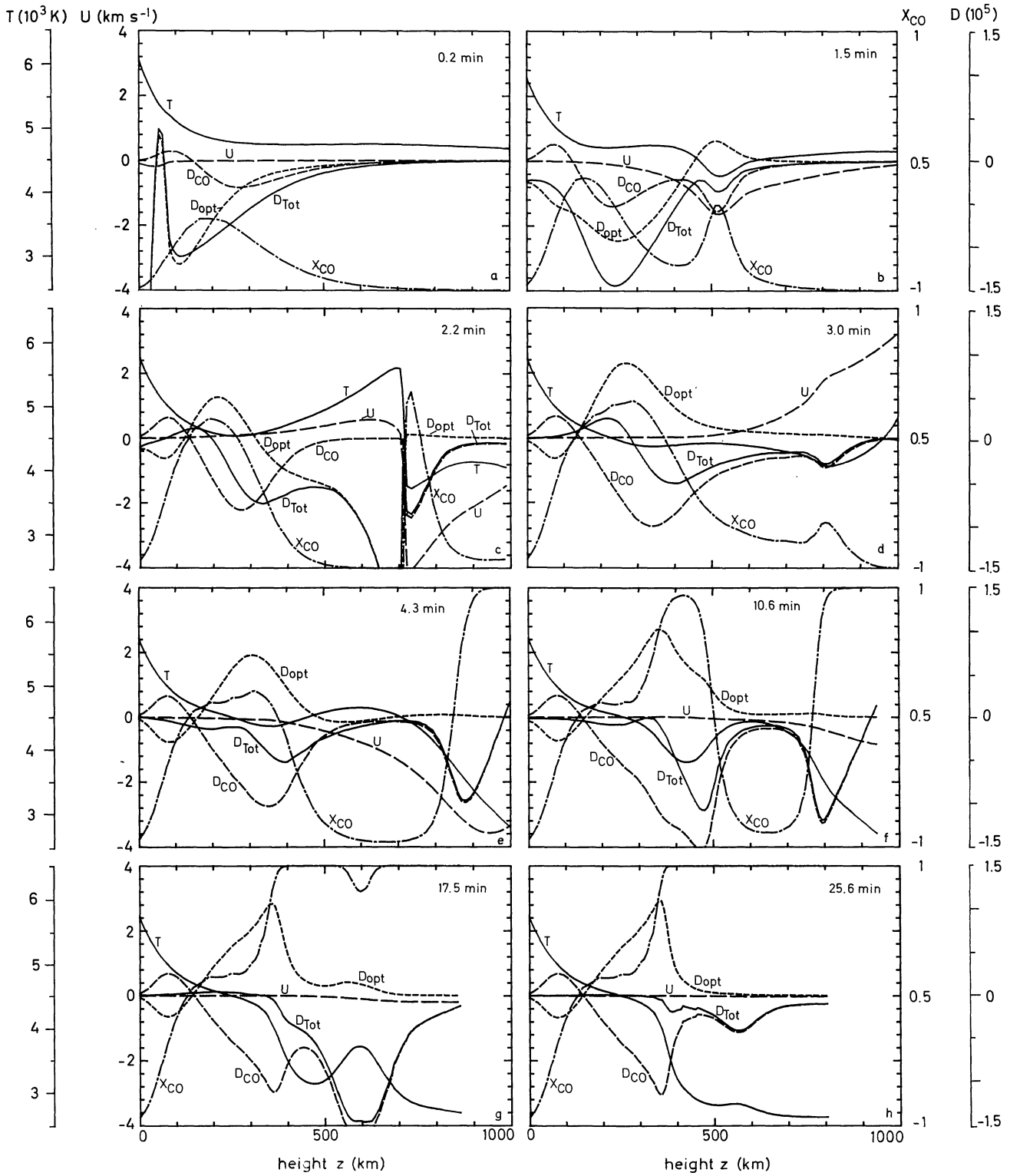

Fig. 5. The evolution of an atmosphere cooling from $T_{\rm eff} = 5900$ to 5600 K due to a sudden decrease in incoming radiation. The radiative damping function $D = \left.\frac{\partial S}{\partial t}\right|_{\rm rad}$ for each of the two frequency bands and the total $D_{\rm Tot} = D_{\rm opt} + D_{\rm CO}$ are plotted together with temperature, T, velocity, u, and the fraction $X_{\rm CO}$ of carbon atoms in CO

The initial response (cf. Fig. 5a) is a rapid radiative cooling in the optical band and contraction in the deepest layers. The reduced pressure there produces a *rarefaction wave* which propagates outward. After 1.5 min (cf. Fig. 5b), the cooling at low photospheric ($z \approx 0$ km) levels has dropped to small values. At large optical depth, radiation adjusts the temperature rapidly. The rarefraction wave at $z = 500$ km reduces the temperature enough for CO to form and in turn acts as a coolant strongly counteracting the radiative heating in the optical band. Moving further out, the wave steepens to a shock, as shown at $t = 2.2$ min (Fig. 5c). In front

of the shock, where T is low, CO acts as a coolant. Behind it where T is high and CO is destroyed, the optical continuum is a coolant, too. Thus the wave accelerates the atmosphere's loss of entropy in both its hot and cool phases. After 3 min (cf. Fig. 5d), the shock has passed out of the top model boundary leaving the shocked gas expanding outwards. The feature seen at $z=850$ km is a reflected wave propagating downwards and is an artifact of our imperfect transmitting boundary condition.

The atmosphere next executes large scale oscillations. At 4.3 min (Fig. 5e) after it has expanded to its maximum value the model now strongly contracts. At the top of the atmosphere ($z=1000$ km) the expansion has reduced the temperature for a long enough time so that CO greatly cools the gas. Henceforth the temperature here stays below 3000 K and all of the carbon is locked up in molecules. A *cooling front* moves inward as radiative losses lead to CO formation and more cooling. Another *cooling front* has been slowly moving outward from the bottom. At about the time this front reaches a height of 400 km, the temperature has dropped enough that CO cooling plays an important role. Note that by the time (4.3 min) of Fig. 5e radiative equilibrium has been established below the height of 300 km. At $t=10.6$ min (cf. Fig. 5f) we see a slowly contracting atmosphere in which oscillations have largely died down and two radiative cooling fronts are gradually approaching each other. They join after about 17.5 min (Fig. 5g) at a height of 600 km. It is these middle altitudes which are the last to cool. Radiative equilibrium is now established up to a height of 400 km. The final frame (Fig. 5h, $t=25.6$ min) of this sequence shows an atmosphere almost in the equilibrium state already discussed. Half an hour has elapsed. The atmosphere has contracted from 1000 km to 800 km and has passed through the instability region shown in Fig. 2.

4.2. *Rate of approach to equilibrium*

The particular example presented above was chosen for the sake of the interesting features which arise during the evolution of the atmosphere. In numerical experiments with smaller perturbations of the boundary conditions, the oscillations in the atmosphere are smaller so that the inward moving cooling front was not generated. In such a case, the outward moving cooling front proceeds more and more slowly at greater heights in the atmosphere. If the initial state has essentially no CO and the equilibrium state would have $X_{CO}\approx 1$, then the temperature at $z=1000$ km remains far from equilibrium for a very long time. We first tried to construct an equilibrium model at $T_{eff}=5770$ K in this way starting with an initial model of $T_{eff}=5900$ K. After 2.2 h, the cooling front had reached $z=630$ km and was moving outward with 13 m s^{-1}. We estimated that to cool the entire atmosphere this way would take over 10 h. The radiative losses were confined to a very narrow layer some 10 km thick. The $T_{eff}=5770$ K equilibrium model was found much more rapidly by starting with a model at $T_{eff}=5600$ K and increasing the incident radiation. A steady radiative heating in the CO band over the entire low temperature plateau at $z>500$ km brought the model into near equilibrium in only 30 min. The approach to radiative equilibrium thus occurs at timescales which depend on the initial state. Consequences of this result for a slowly fluctuating granulation field will be investigated in a separate paper.

4.3. *Atmospheres with mechanical heating*

The models discussed so far are unrealistically quiescent. Turbulent flow fields like the solar convection zone cannot avoid generating acoustic energy. The amount of mechanical energy although still debated (Deubner, 1976; Deubner et al., 1982; Bohn, 1984) is appreciable, while magnetic fields act to further enhance the acoustic energy production (Ulmschneider and Stein, 1982). It thus appears that realistic atmosphere models should include heating processes other than radiative transfer. Figure 3 shows the response of the mean atmosphere (time averaged over one wave period) to wave propagation and mechanical heating of a model initially in radiative equilibrium at $T_{eff}=5770$ K after various amounts of acoustic energy are introduced. We have adopted cases of moderately high and low acoustic flux by assuming $F_M=1\,10^8$ and $1\,10^7$ erg cm^{-2} s^{-1}, respectively.

After a timespan of about 20 min the atmospheres have reached a dynamical steady state, that is, the mean temperatures did not show changes with time anymore. It is interesting to note that even in the higher acoustic flux case the very deep temperature minimum around $T=3200$ K remains at $z=500$ km. For the low flux case the minimum has a value of $T=3000$ K at $z=650$ km. These minima always occurred close to the height of shock formation.

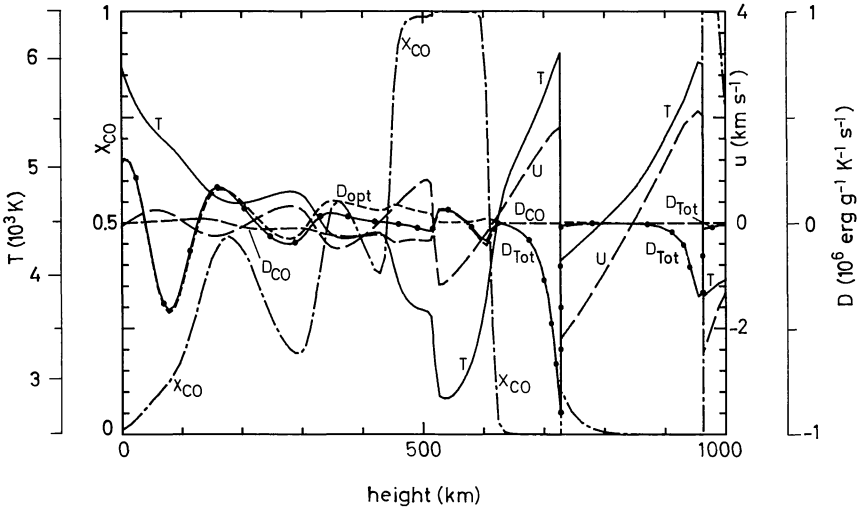

Fig. 6. Physical conditions in an atmosphere permeated by an acoustic wave of period 30 s and energy flux $1\,10^8$ erg cm^{-2} s^{-1} at time 27 min, $T_{eff}=5770$ K. The phase of this snapshot corresponds to the moment where a shock i formed near the height $z=500$ km. The quantities plotted are the same as in Fig. 5, but note that the scale for D is expanded

The processes which limit the extent of the CO-dominated region are most clearly seen in Fig. 6 which shows the physical variables in a wave moving through the atmosphere. Here the wave of higher energy is displayed at time $t=27$ min where the 51 st shock has just formed at height $z=500$ km. Below that height one has radiative equilibrium perturbed by the wave. As discussed above the CO-dominated region (cf. Fig. 4) begins when the CO-optical depth drops below unity and CO-cooling becomes important. Figure 6 shows that the CO-region ends as soon as the shock has gained appreciable strength at a height of roughly one half wavelength above shock formation where the heating destroys the CO molecule. From this point up into the chromosphere H^- is the dominant cooling mechanism. [For a discussion of wave propagation in an atmosphere dominated by H^- see Schmitz et al. (1984).]

As an increasing acoustic flux decreases the height of shock formation it is clear that there is a critical mechanical flux $F_{M_{cr}}$ of about $5\,10^8$ erg cm^{-2} s^{-1} where shock dissipation occurs below the height of $z\approx 400$ km at which CO becomes appreciable. In such cases of very high mechanical energy flux CO would not play an appreciable role anymore in the atmosphere. This agrees well with the scenario developed by Ayres (1981). For acoustic fluxes $F_M < F_{M_{cr}}$ a cool CO-dominated temperature minimum region develops which becomes more extended the smaller F_M is (cf. Fig. 3).

5. Discussion and conclusions

With a time-dependent method we have simulated the influence of CO on H^- – dominated atmospheres of stars with solar type gravity and effective temperatures. Assuming LTE and a plane-parallel, two-frequency band treatment of the radiation field we have calculated the time evolution of model atmospheres for cases of different incident radiation fields, with and without mechanical heating. We found that contrary to the speculation of Kneer (1983) all cases without mechanical heating approached radiative equilibrium atmospheres (cf. Figs. 4 and 5). All cases with mechanical heating developed into dynamical steady state models.

Our calculations clearly show the bistable thermal structure described by Ayres (1981). Optically thin gas in a stellar atmosphere tends to be unstable between 3500 and 4500 K (Figs. 2, and 3). We find critical effective temperatures $T_{cr}\approx T'_{cr}\approx 5800$–$5900$ K, such that radiative equilibrium atmospheres with $T_{eff} > T'_{cr}$ remain above the unstable temperature range while atmospheres with $T_{eff} < T_{cr}$ fall below this range (Fig. 3). For models with $T_{eff}=5770$ K the outer boundary temperature drops to about 3100 K which is considerably below even the cold CO line cores seen by Ayres and Testerman (1981).

Heating the atmospheres with small or moderately large amounts of acoustic energy did not prevent the occurence of a cold CO-dominated temperature minimum region (Figs. 3 and 6). This region extends roughly from the height, where the CO-optical depth drops below one to a level somewhat above the height of shock formation, where mechanical dissipation becomes appreciable and CO is destroyed. As the shock formation heights decrease with increasing acoustic energy flux, there is a critical flux $F_{M_{cr}}$ $\approx 5\,10^8$ erg cm^{-2} s^{-1} where CO ceases to play an influence in the atmosphere. This property is in good agreement with the scenario proposed by Ayres (1981).

The time scale for establishment of radiative equilibrium below the height of $z=1000$ km is of the order of one hour if the thermal equilibration is aided by dynamical effects. However, for small changes of the incident radiation field the atmosphere comes to equilibrium less by dynamical but more by radiative processes. If in this case the equilibration involves crossing between the CO-dominated state (at $T\leqq 3500$ K) and the hotter state (at $T>4500$ K) the time scale can be an order of magnitude larger. Both time scales are long compared to typical granulation time scales of 16 min. This shows that the solar atmosphere above $z=400$ km does not appear to be in an equilibrium state at any one time.

The two-frequency-band method used here leaves much to be desired. The CO opacity is smeared smoothly over a broad frequency band. Treating a series of line-opacities as a single continuum opacity is a suspect procedure when the opacities in the different lines are unequal and the line cores are not optically thin. In addition, to describe the temperature minimum region realistically, the radiative calculation should also include non-LTE effects in H^- and atomic lines. Here it suffices to say that in calculations presently planned we want to include effects of departures from LTE in H^-, Mg II, and Ca II and attempt to treat the CO-band with opacity distribution functions.

Another crucial question which we have not discussed here is the rate of molecular association-dissociation reactions. Using Henning's (1981) rate for the reaction $CH+O\rightarrow CO+H$, and Tatum's (1966) equilibrium constants for CH and CO at 6000 K, yields a rate for the reverse reaction of $d\ln N_{CO}/dt = 2\,10^{-15}$ N_H cm^3 s^{-1}. At the densities of $N_H\sim 10^{13}$–10^{14} cm^{-3} occuring near $z=1000$ km in these models, the implied destruction time through this one reaction alone is 5–50 s. At the same time, of course, other reactions both create and destroy CO, so that the net destruction rate may be rather different. This one rate is enough to show that our LTE assumption is not warranted in the outer parts of the models when conditions change much faster. At $z=500$ km, densities are two orders of magnitude higher and the CO abundance should reflect LTE.

The very low outer temperatures that CO emission produces in radiative equilibrium atmospheres may lead to further effects that were not included here. In a gas at $T<3200$ K water vapor becomes the dominant source of opacity (Alexander et al., 1983). It should act as a coolant just as CO does. A true radiative equilibrium atmosphere in a solar-type star would then be even colder than our models.

Acknowledgement. We are glad to acknowledge the support of the Deutsche Forschungsgemeinschaft (SFB 132).

References

Alexander, D.R., Johnson, H.R., Rypma, R.L.: 1983, *Astrophys. J.* **272**, 773
Ayres, T.R.: 1980, *Solar Phys.* **68**, 125
Ayres, T.R.: 1981, *Astrophys. J.* **244**, 1064
Ayres, T.R., Linsky, J.L.: 1976, *Astrophys. J.* **205**, 874
Ayres, T.R., Testerman, L.: 1981, *Astrophys. J.* **245**, 1124
Bohn, H.U.: 1984, *Astron. Astrophys.* (in press)
Deubner, F.: 1976, *Astron. Astrophys.* **51**, 189
Deubner, F., Durrant, C.J., Kaltenbacher, J.: 1982, *Astron. Astrophys.* **114**, 85
Henning, K.: 1981, *Astron. Astrophys.* **44**, 405
Huber, K.P., Herzberg, G.: 1979, Molecular Spectra and Molecular Structure, Vol. IV, Van Nostrand

Kalkofen, W., Ulmschneider, P.: 1977, *Astron. Astrophys.* **57**, 193
Kirby-Docken, K., Liu, B.: 1978, *Astrophys. J. Suppl.* **36**, 359
Kneer, F.: 1983, *Astron. Astrophys.* **128**, 311
Kurucz, R.: 1979, *Astrophys. J. Suppl.* **40**, 1
Kurucz, R.: 1983 (private communication)
Mihalas, D.: 1978, Stellar Atmospheres, Freeman, San Francisco
Noyes, R.W., Hall, D.N.B.: 1972, *Astrophys. J.* **176**, L89
Schmitz, F., Ulmschneider, P., Kalkofen, W.: 1984, *Astron. Astrophys.* (to be published)
Tatum, J.B.: 1966, *Publ. Dominion Astrophys. Obs. XII*, No. 1
Thompson, R.I.: 1973, *Astrophys. J.* **181**, 1052
Tsuji, T.: 1964, *Ann. Tokyo Astron. Obs.* **9**, 1
Ulmschneider, P.: 1984 (in preparation)
Ulmschneider, P., Kalkofen, W., Nowak, T., Bohn, U.: 1977, *Astron. Astrophys.* **54**, 61
Ulmschneider, P., Schmitz, F., Kalkofen, W., Bohn, H.U.: 1978, *Astron. Astrophys.* **70**, 487
Ulmschneider, P., Stein, R.F.: 1982, *Astron. Astrophys.* **106**, 9
Vernazza, J.E., Avrett, E.H., Loeser, R.: 1981, *Astrophys. J. Suppl.* **45**, 635